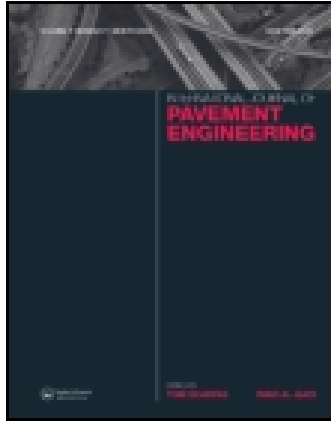


This article was downloaded by: [Eindhoven Technical University]

On: 14 February 2015, At: 20:16

Publisher: Taylor & Francis

Informa Ltd Registered in England and Wales Registered Number: 1072954 Registered office: Mortimer House, 37-41 Mortimer Street, London W1T 3JH, UK



## International Journal of Pavement Engineering

Publication details, including instructions for authors and subscription information:

<http://www.tandfonline.com/loi/gpav20>

### Analysis of Load Responses in PCC Airport Pavement

Yingwu Fang <sup>a</sup>

<sup>a</sup> LAW PCS , 12104 Indian Creek Court , Suite A., Beltsville, MD, 20705-1242, USA

Published online: 01 Feb 2007.

To cite this article: Yingwu Fang (1999) Analysis of Load Responses in PCC Airport Pavement, International Journal of Pavement Engineering, 1:1, 1-14, DOI: [10.1080/10298439908901693](https://doi.org/10.1080/10298439908901693)

To link to this article: <http://dx.doi.org/10.1080/10298439908901693>

PLEASE SCROLL DOWN FOR ARTICLE

Taylor & Francis makes every effort to ensure the accuracy of all the information (the "Content") contained in the publications on our platform. However, Taylor & Francis, our agents, and our licensors make no representations or warranties whatsoever as to the accuracy, completeness, or suitability for any purpose of the Content. Any opinions and views expressed in this publication are the opinions and views of the authors, and are not the views of or endorsed by Taylor & Francis. The accuracy of the Content should not be relied upon and should be independently verified with primary sources of information. Taylor and Francis shall not be liable for any losses, actions, claims, proceedings, demands, costs, expenses, damages, and other liabilities whatsoever or howsoever caused arising directly or indirectly in connection with, in relation to or arising out of the use of the Content.

This article may be used for research, teaching, and private study purposes. Any substantial or systematic reproduction, redistribution, reselling, loan, sub-licensing, systematic supply, or distribution in any form to anyone is expressly forbidden. Terms & Conditions of access and use can be found at <http://www.tandfonline.com/page/terms-and-conditions>

# Analysis of Load Responses in PCC Airport Pavement

YINGWU FANG\*

LAW PCS, 12104 Indian Creek Court, Suite A, Beltsville, MD 20705-1242, USA

(Received January 25, 1999; Revised June 15, 1999)

To understand what actually happens in the pavement as aircraft wheels pass by, pavement deflections and strains were plotted against time using field test data collected at Denver International Airport. Shapes of the response-versus-time curves were analyzed in detail, and the locations of the maximum responses are shown graphically.

According to the analysis, maximum deflections occur between the dual wheels, whereas maximum strains occur beneath one of the wheels. The plots also show clear reversals in the longitudinal strain-versus-time curves. These strain reversals were carefully investigated and some interesting results were obtained. A method to compute the deflection-based load transfer efficiencies was developed. The computation further showed that the load transfer efficiency for dummy joints is direction dependent, and that the load transfer efficiency decreases significantly during the first year the pavement is in service.

**Keywords:** Portland Cement Concrete pavement, Deflection, Strain, Pavement response, Sensor

## BACKGROUND

The test area built by the FAA Technical Center at the new Denver International Airport is composed of 16 PCC pavement slabs forming a rectangular test area 4 slabs by 4 slabs. Each slab is 6.10 m in length, 5.72 m in width, and 46 cm in thickness. The slabs were constructed on top of a 20-cm thick cement-treated base and a 30-cm thick lime-stabilized subbase. More than 200 dynamic sensors were embedded in the pavement layers. These include 100 H-Bar strain gages and 23 Carlson strain gages to measure horizontal strains at different depths within and below the PCC pavement; 50 Linearly Variable Differential Transformer (LVDT) sensors to measure vertical displacements of the pavement slabs and the lower layers; 7 IR sensors (photoelectric eye sensors) to measure the longitudi-

nal position of the aircraft; and 36 position strain gages to measure the transverse location of the wheels (Dong et al. (1997)).

The data acquisition system is triggered automatically when the departing aircraft runs over the test area. Test data are stored in a computer hard drive in binary format, and processed periodically using a Visual Basic computer program. Peak responses and typical peak records (response-versus-time curves) are loaded into an Oracle database (FAA Internet site). The objective of this paper is to analyze the shapes of the deflection and strain peak records to find out what is actually occurring in the pavement. The analysis was done qualitatively, rather than quantitatively. Three typical aircraft types were selected for the analysis. These included the B-777, DC-10,

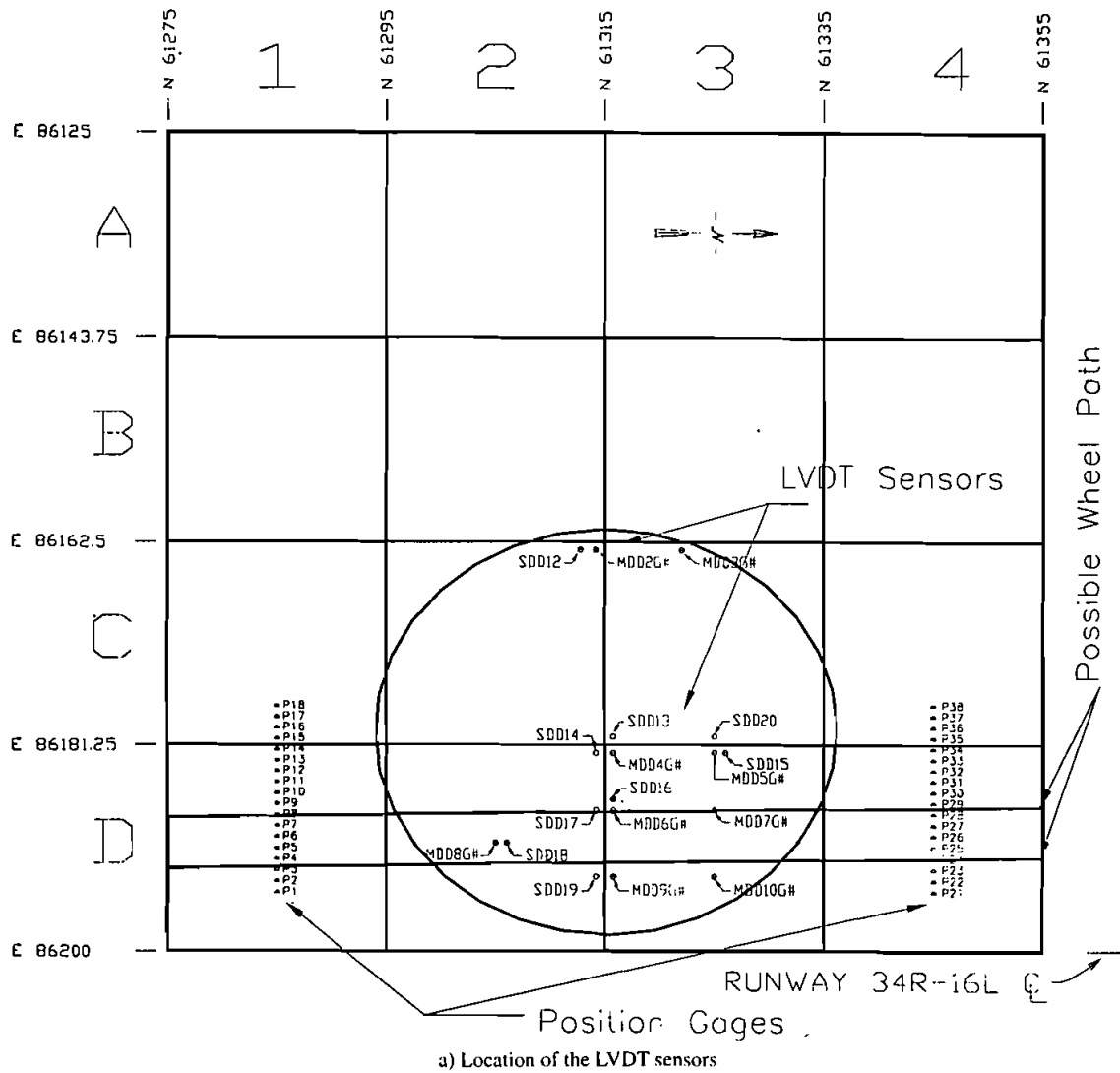
\* Email: yfang@lawco.com

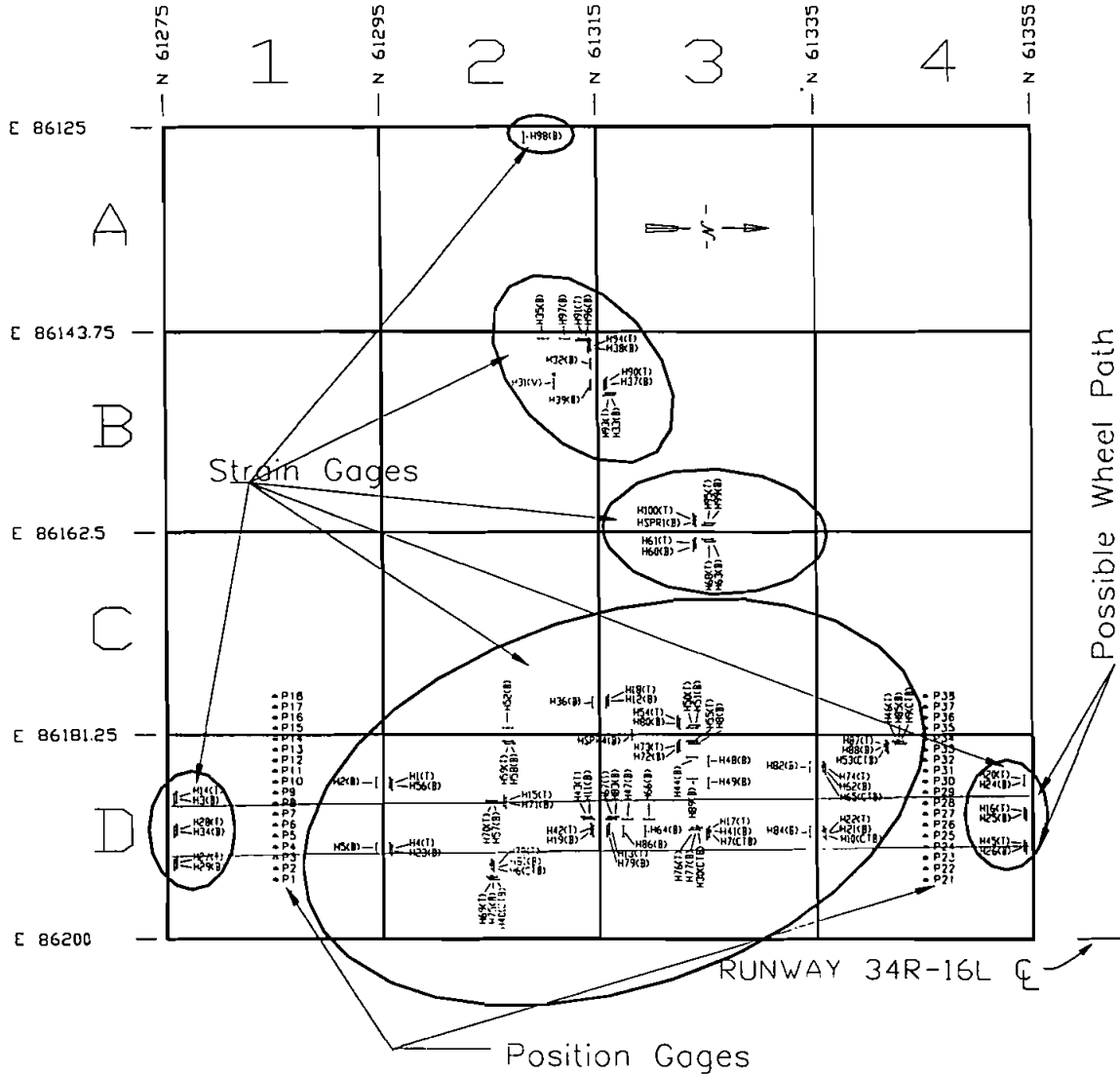
and B-727. These aircraft types were chosen because they represent the three major main gear configurations in commercial aircraft.

**LOCATION OF LVDT AND STRAIN GAGES**

As shown in Fig. 1a, two types of LVDT sensors were instrumented in this test runway: single depth deflectometers (SDD) and multidepth deflectometers (MDD). The SDD and MDD sensors were retrofitted into the pavement layers. Each MDD sensor has 4

LVDT modules. The modules are located at 1) about the mid-depth location of the PCC pavement slab, 2) the bottom of the cement-treated base, 3) the bottom of the lime-treated subbase, and 4) 0.30 m below the top of the subgrade. The SDD sensors each have one LVDT module imbedded at about the mid-depth location of the PCC pavement slabs. The measured displacements are in terms of the relative movement between the LVDT and the anchor, which is at a fixed depth from the LVDT (6.10 m and 3.05 m from the top surface of the PCC pavement slab for SDD and MDD sensors, respectively).





b) Location and direction of the strain sensors

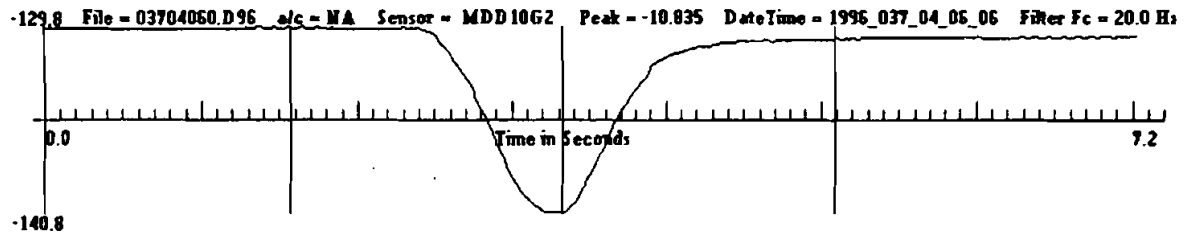
FIGURE 1 Location of LVDT and strain gages

The locations of the H-Bar strain gages are shown in Fig. 1b. The gages were imbedded at different depths, including the top and bottom surfaces of the PCC slabs, to measure horizontal strains in both the longitudinal and transverse directions (FAA Internet site).

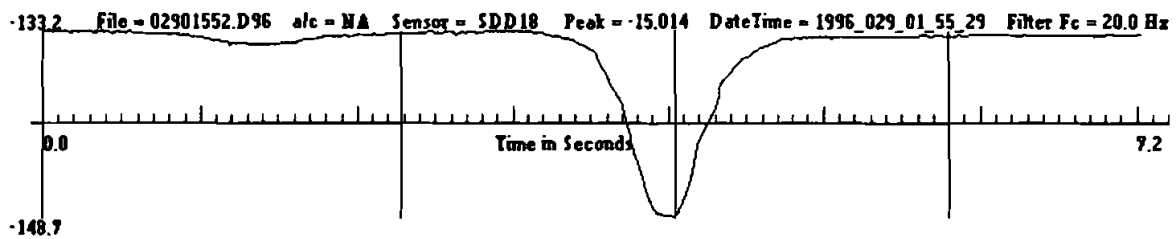
**SHAPES OF DEFLECTION CURVES**

**Case 1: Wheels Are Midway between Transverse Joints**

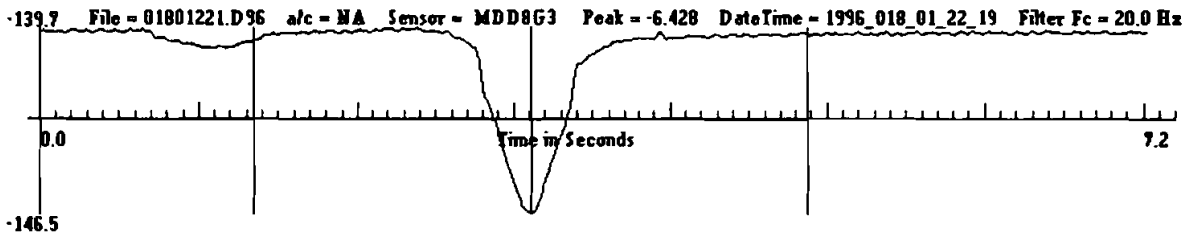
This situation applies to both the inner loading case and the longitudinal joint loading case. The sensors at



a For B-777 Gear



b For DC-10 Gear



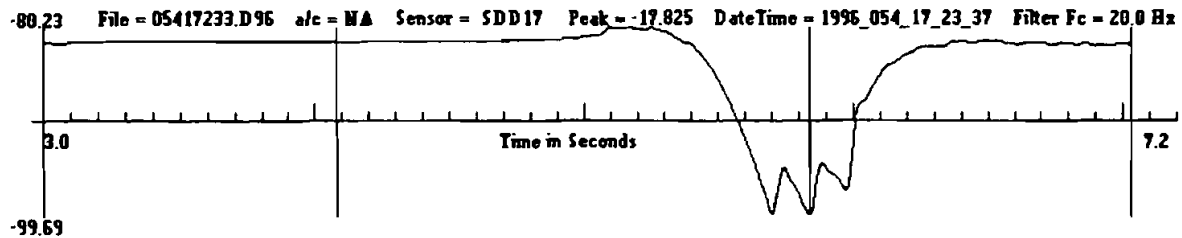
c For B-727 Gear

FIGURE 2 Deflection (mil) versus time curves for the inner loading case

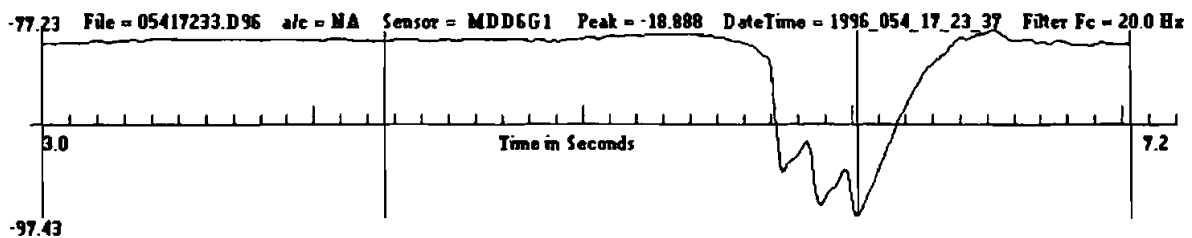
these locations include MDD8, SDD18, MDD10, and MDD7. Data collected by these sensors were used to plot the deflection versus time curves, as shown in Fig. 2. For a better comparison, the three curves were plotted on the same time scale.

The following findings are observed from these curves:

- **Symmetry:** All three curves are smooth and approximately symmetrical, which indicates that the direction in which the aircraft was operated did not affect the shape of the curves.
- **Sharpness:** As expected, the curve for the DC-10 gear is sharper (peak record covers a narrower time range) than the one for the B-777 gear and the curve for the B-727 gear is sharper than the one for the DC-10 gear. This is because the DC-10 gear has one less main gear axle than the B-777 gear and the B-727 gear has one less main gear axle than the DC-10 gear. The load is more concentrated with fewer main gear axles.
- **Number of peaks:** Although the B-777 gear and the DC-10 gear have more than one main gear



a On the south side of the transverse joint



b On the north side of the transverse joint

FIGURE 3 Deflection (mil) versus time curves for B-777 (2/96)

axle, the deflection versus time curves each have only one peak.

- **Location of maximum deflection:** The maximum deflection occurred beneath the middle axle for the B-777 gear, midway between the two main gear axles for the DC-10 gear, and beneath the single axle for the B-727 gear, respectively.

### Case 2: Wheels Are at the Transverse Joints

The measurements of SDD17, SDD19, SDD16, MDD6, and MDD9 sensors were used to plot the deflection versus time curves for the edge loading case at the transverse joints. Figs 3–5 show the deflection versus time curves for the edge loading case for each of the three selected aircraft types.

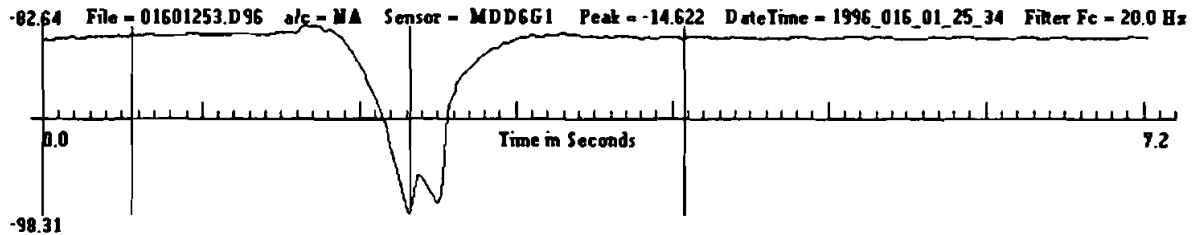
Similarly, the following are the findings observed from the above curves:

- **Non-symmetry:** All the curves are no longer symmetrical due to the existence of the transverse joints.

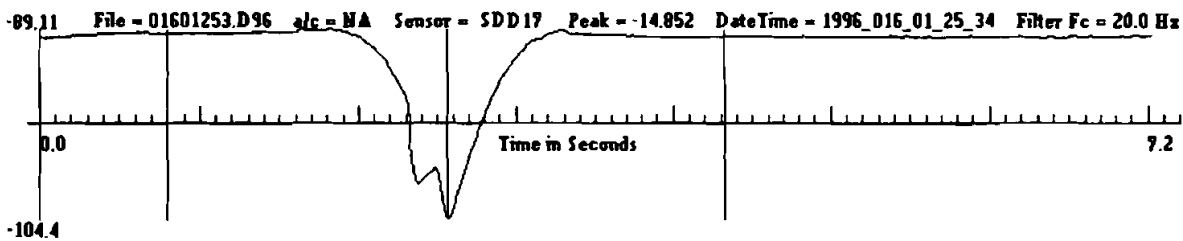
- **Sharpness:** The curve representing aircraft with fewer main gear axles covers a narrower time range.
- **Number of peaks:** In contrast with the inner loading case, the deflection versus time curves at the transverse joint have the same number of peaks as the number of the main gear axles of the aircraft. That is, the deflection versus time curve at the transverse edge of the slabs has three peaks for the B-777 gear, two peaks for the DC-10 gear, and one peak for the B-727 gear.
- **Location of maximum deflection:** The maximum deflection peak can occur below any main gear axle, depending on the joint load transfer characteristics.

### DIRECTION-DEPENDENT LOAD TRANSFER EFFICIENCIES

Since each pair of Figs 3–5 were plotted for the same aircraft operation and on the same time scale, they can



a On the south side of the transverse joint



b On the north side of the transverse joint

FIGURE 4 Deflection (mil) versus time curves for DC-10 Gear (1/96)

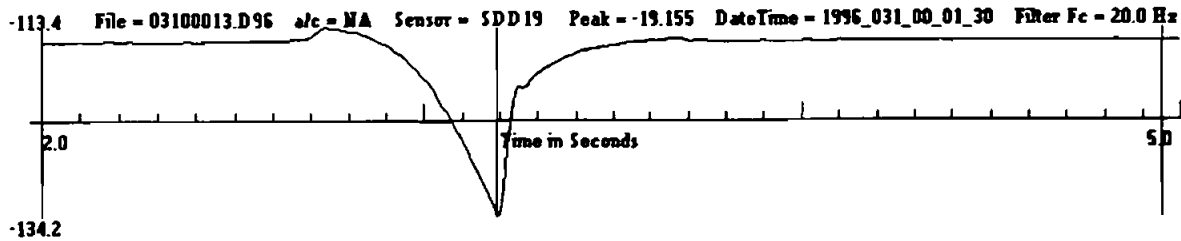
be used to analyze load transfer characteristics of the joint. If the load transfer efficiency is independent of the direction in which the aircraft was operated, the pair of figures should approximately mirror each other. However, this is not the case, as seen in Fig. 3. The two curves are different in the following respects:

- The maximum peak on the south side of the joint was triggered by the middle main gear axle, but the one on the north side was triggered by the rear main gear axle.
- The peaks triggered by the front and middle axles on the south side of the joint were close in magnitude, but there was a clear difference between the deflections triggered by the middle and rear axles on the north side of the joint.

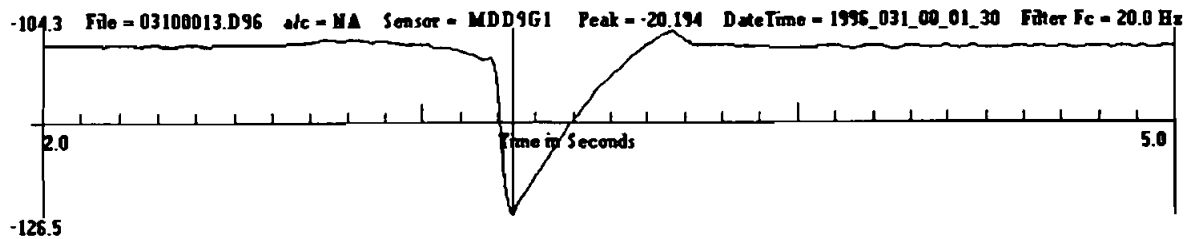
This could be attributed to the difference in load transfer efficiencies. It means that the load transfer efficiency to transfer load from the south side slab to the north side one is different from that if the load is transferred in the opposite direction.

To further prove the above justification, the deflection versus time curves in Fig. 5 for a B-727 operation were analyzed. A scheme was developed to compute the load transfer efficiency values based on the measured deflections.

First, the exact time when the peaks occurred was obtained in the horizontal time axis. Then the deflection values at the time were measured from both curves. The load transfer efficiency for transferring load from the south side slab to the north side slab is equal to the deflection measured in Fig. 5b at the time when the peak in Fig. 5a occurred divided by the peak deflection in Fig. 5a. The load transfer efficiency for transferring load from the north side slab to the south side slab can be obtained similarly. The load transfer efficiency thus obtained was 20% for transferring load from the south side slab to the north side slab, and 15% if it was done in the opposite direction. The difference between the two values was due to the irregular development of the undowelled dummy joint, as shown in Fig. 6.



a On the south side of the transverse joint



b On the north side of the transverse joint

FIGURE 5 Deflection (mil) versus time curves for B-727 (1/96)

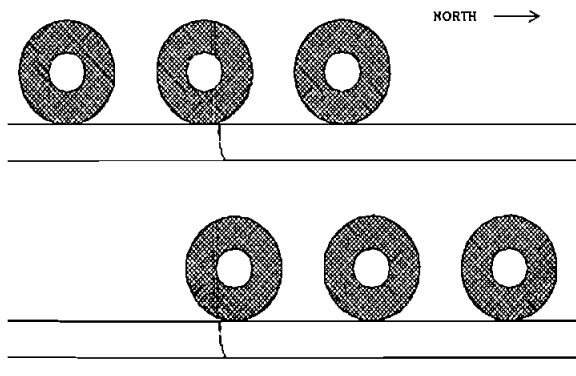


FIGURE 6 Irregular development of dummy joint

These computed load transfer efficiencies were very low due to two reasons: the joint was undowelled and the values were measured in the winter (January 16, 1996) when the pavement slabs had contracted. Actually, these deflection values were measured just one year after the new runway was open for operation. In order to find out what the load

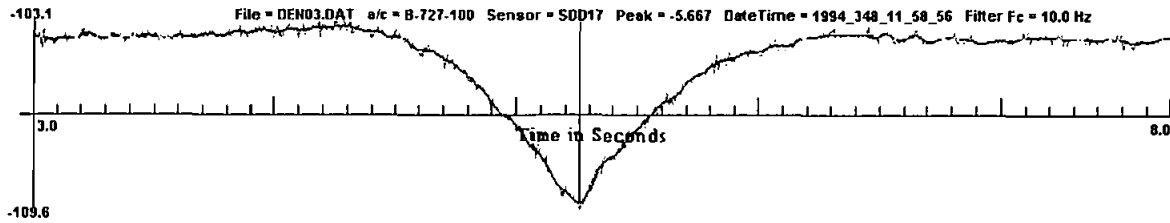
transfer efficiencies originally were, similar deflection versus time curves were plotted for a B-727 operation performed on December 14, 1994 before the runway was open for operation, as shown in Fig. 7. In this figure, load transfer efficiency was found to be 85% for transferring load from the south side slab to the north side slab and 78% if it was done in the opposite direction. Since both tests were carried out in the winter, the seasonal effect was eliminated. It can be seen that load transfer efficiency has decreased a lot in a little over one year. This is a major drawback of undowelled dummy joints.

## SHAPES OF STRAIN CURVES

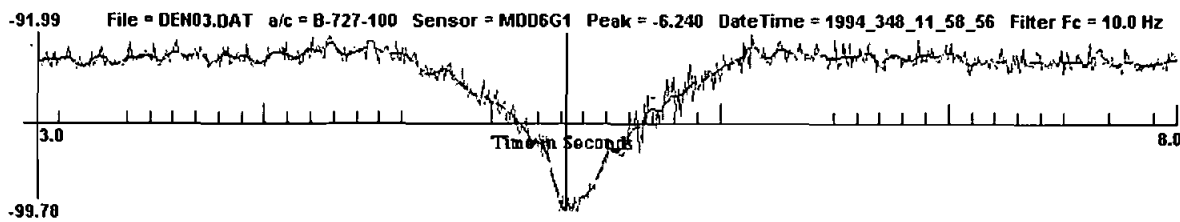
### Case 1: Wheels Are Midway between Transverse Joints

Figure 8 shows the strain versus time curves for the case of a B-777 operation. The two curves were plot-



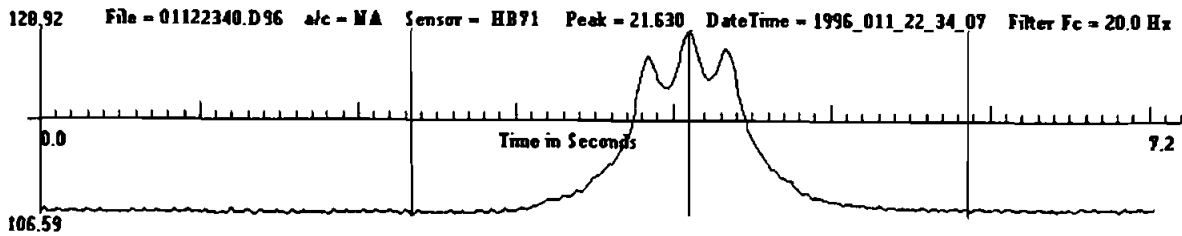


a On the south side of the joint

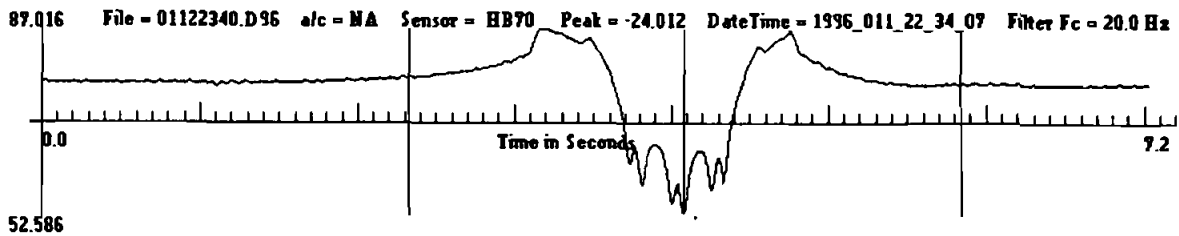


b On the north side of the joint

FIGURE 7 Load transfer characteristics for B-727 (12/94)



a Transverse strain versus time curve



b Longitudinal strain versus time curve

FIGURE 8 Strain ( $\mu\epsilon$ ) versus time curves for the inner loading Case for B-777

ted for the same lateral location. Figure 8a shows a transverse strain versus time curve at the depth of 2.54 cm from the bottom of the PCC layer and Figure 8b shows a longitudinal strain versus time curve at the depth of 9.09 cm from the top surface of the PCC layer. In contrast with the deflection versus time curves for the inner loading case, these strain versus time curves have three peaks for the B-777 gear, triggered by each axle respectively. Both curves are approximately symmetrical. The maximum strain occurred below the middle axle of the B-777 main gear.

Similar analysis was done for other two selected aircraft types: DC-10 and B-727. The following findings were observed:

- **Symmetry:** When the wheels are away from the transverse joints, both the transverse strain curve and the longitudinal strain curve were symmetrical. The maximum strain occurred below the middle axle of the B-777 gear, below either of the two main gear axles for the DC-10 gear, and below the single main gear axle for the B-727 gear.

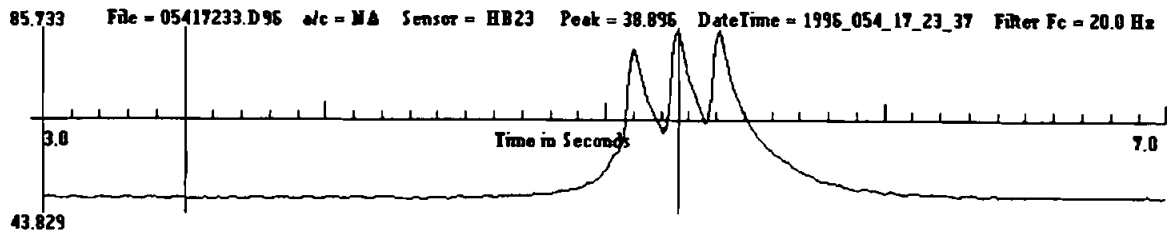
- **Number of peaks:** The strain versus time curves for the inner loading case have the same number of peaks as the number of the main gear axles of the aircraft, triggered by each axle respectively.
- **Curvature changes:** The longitudinal strain versus time curve shows more complicated curvature changes for all the three selected aircraft types.

### Case 2: Wheels Are at the Transverse Joints

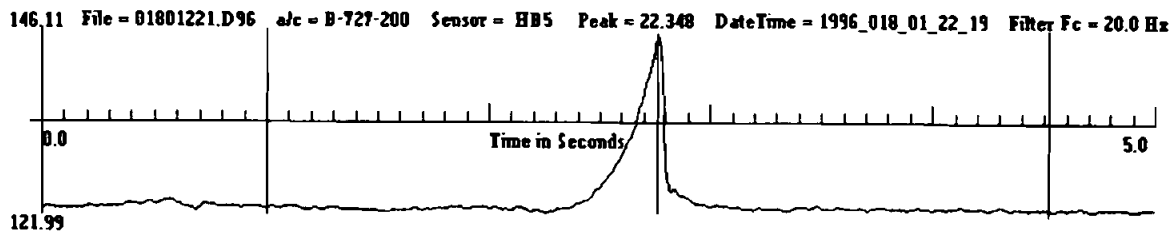
To save space, only two typical strain versus time curves were plotted, as shown in Fig. 9.

Again the findings can be concluded as follows:

- **Non-symmetry:** The transverse strain curve at the transverse edge of the slab is no longer symmetrical.
- **Number of peaks:** The strain versus time curves for the edge loading case have the same number of peaks as the number of the main gear axles of the aircraft, triggered by each axle respectively.



a Transverse strain at transverse edge for B-777



b Transverse strain at transverse edge for B-727

FIGURE 9 Strain ( $\mu\epsilon$ ) versus time curves for the edge loading case

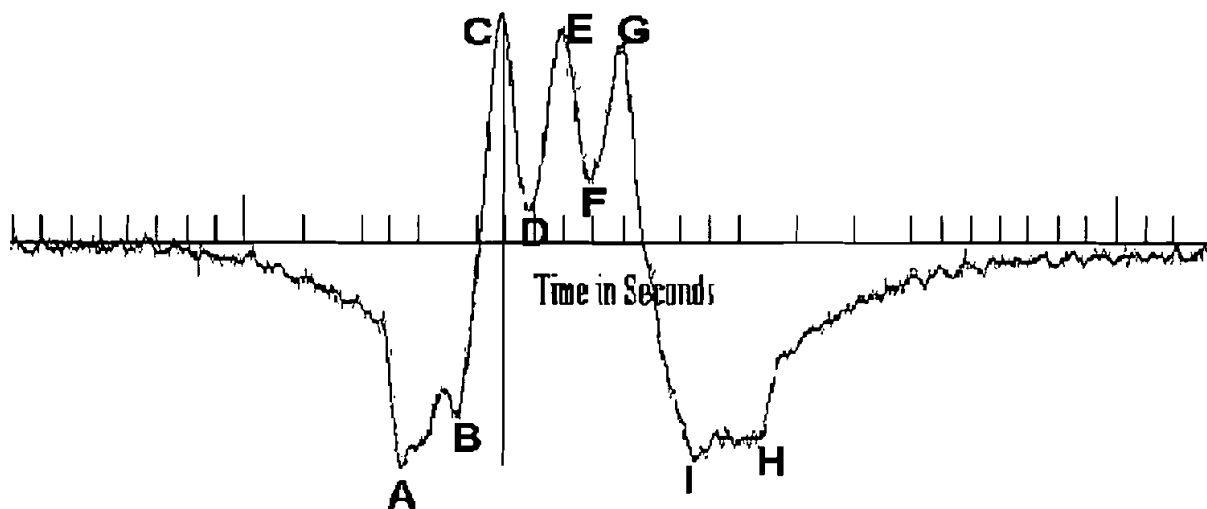


FIGURE 10 Curvature changes (strain versus time plot)

### STRAIN REVERSALS AND THEIR EFFECTS ON PAVEMENT LIFE

As shown in the above analysis, pavements along the wheel path are subjected to full strain reversals as the aircraft wheels move in the longitudinal direction of the runway. At the top surface of the pavement, the slab concrete is subjected to tensile strains when the wheels approach the evaluation location, compressive strains when the wheels are at the evaluation location and tensile strains again when the wheels leave but are still close to the location. Fig. 10 shows part of a strain versus time curve for a B-777, and the locations where significant curvature changes occurred are marked alphabetically using capital letters.

The times when these curvature changes occurred were read from the original curve. In the figure, the time duration between C and G is the period during which the aircraft traveled a distance between the first and the third axles of the main gear. Hence the speed of the aircraft can be estimated by dividing this distance, which is 2.9 m, by the related time period:

$$2.9/(4.31-3.90)=7.07 \text{ (m/second)}$$

TABLE I Distance calculation

Section	Time duration (second)	Distance traveled (m)
Between A and C	$3.90 - 3.54 = 0.36$	$7.07 \times 0.36 = 2.55$
Between A and B	$3.75 - 3.54 = 0.21$	$7.07 \times 0.21 = 1.48$
Between G and H	$4.80 - 4.31 = 0.49$	$7.07 \times 0.49 = 3.46$
Between I and H	$4.80 - 4.58 = 0.22$	$7.07 \times 0.22 = 1.56$

The distances the aircraft traveled during the other time periods can be calculated by multiplying the corresponding time difference with the estimated speed of the aircraft, as shown in Table I.

The data were collected by strain gage HB58 that was imbedded along the longitudinal joint, approximately midway from the two adjacent transverse joints, and at the bottom of the PCC slab. The following findings about the estimated distances in Table I are quite interesting:

- The distance between A and C is very close to the distance from the north side transverse joint to the sensor location, which is 2.59 m.

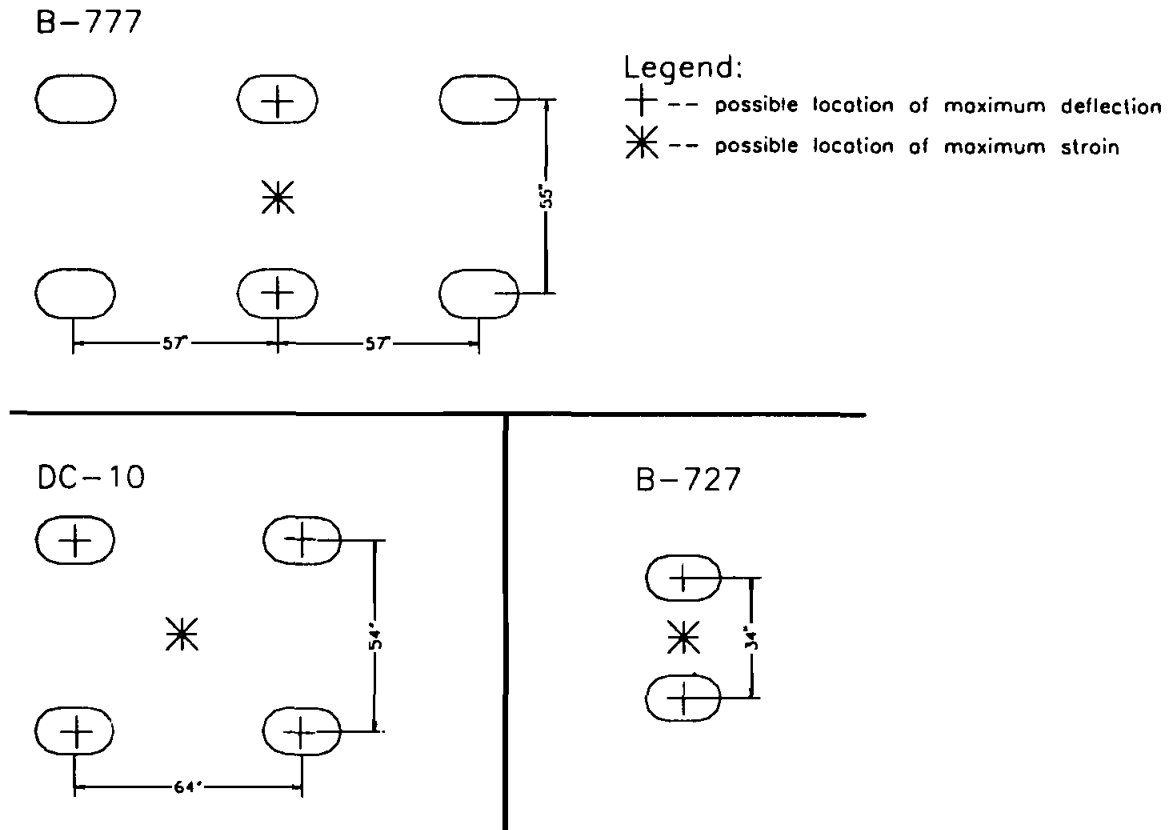


FIGURE 11 Critical deflection and strain locations for the inner loading case

- The distance between *G* and *H* is very close to the distance from the south side transverse joint to the sensor location, which is 3.51 m.
- The distance between *A* and *B* and the distance between *I* and *H* are close to the distance between two adjacent main gear axles for Boeing 777 aircraft, which is 1.45 m.

This was a landing aircraft heading south. Considering the fact that the distance between *A* and *C* is approximately the distance from the north side transverse joint to the sensor location and the fact that the peak at *C* occurred when the first main gear axle was at the sensor location, it can be easily found that the curvature change at *A* in Fig. 10 occurred when the first main gear axle of the B-777 aircraft reached the

edge of the slab on the north side. Since the distance between *A* and *B* is approximately the distance between two adjacent main gear axles for Boeing 777 aircraft, it can be concluded that the curvature change at *B* occurred when the second main gear axle reached the slab edge on the north side. The three peaks were triggered when the three main gear axles pass over the sensor location. Similarly, by comparing the estimated distances, it was found that the curvature change at *I* occurred when the second main gear axle of the B-777 aircraft left the edge of the slab on the south side. The curvature change at *H* occurred when the second main gear axle of the B-777 aircraft left the edge of the slab on the south side.

TABLE II Comparison of deflection and strain values

<i>Time when data were collected</i>	<i>Sensor</i>	<i>Sensor location</i>	<i>Peak deflection</i>
17:23 GMT, Feb. 23, 96	MDD7G1 (deflection)	Inner loading, beneath wheel	8.91 (mil)
	MDD8G1 (deflection)	Inner loading, between wheels	11.83 (mil)
22:34 GMT, Jan. 11, 96	SDD17 (deflection)	Transverse joint, beneath wheel	18.18 (mil)
	SDD16 (deflection)	Transverse joints, between wheels	23.49 (mil)
	H4 (strain)	Transverse joints, top of PCC slab, beneath wheel	-34.57 (microstrain)
	H42 (strain)	Transverse joints, top of PCC slab, between wheels	-19.45 (microstrain)
	H23 (strain)	Transverse joints, bottom of PCC slab, beneath wheel Transverse joints,	38.90 (microstrain)
22:34 GMT, Jan. 11, 96	H19 (strain)	bottom of PCC slab, between wheels Inner loading,	20.89 (microstrain)
	A6547 (strain)	longitudinal strain, bottom of PCC slab, beneath wheel	13.27 (microstrain)
	A6522 (strain)	Inner loading, longitudinal strain, bottom of PCC slab, between wheels	9.98 (microstrain)

The above findings mean that part of the slab around the sensor location started to bend upward once the first axle of the aircraft reached the slab on the north side in which the sensor is imbedded. This upward bending continued until the second axle of the aircraft reached the slab edge. The slab then started to bend towards the opposite direction sharply until the first axle is right above the sensor, when the longitudinal horizontal strains reached the first peak. As the aircraft moved forward, the bending was reversed a few times and two more strain peaks were triggered in the slab when the second and third axles of the gear were right above the sensor. After the third peak, the bending at the sensor location was changed from downward bending to upward bending sharply and two more significant curvature changes occurred when the second and third axles of the gear left the slab on the south side.

In Fig. 10, the strain versus time curve has two compressive peaks before and after the tensile peaks. This causes full reversals of the longitudinal strains in the pavement slab. Similarly, if the data collected by the sensors imbedded close to the top of the PCC slabs are used to plot the curves, two tensile strain peaks are found. This raises the question: Is it possible that these tensile strains of this magnitude can cause surface fatigue of the pavement? Taking into account three important facts, the answer to this question could be "yes". These facts are:

- The values of the reversed strain can be comparable in value to the maximum peak strain, especially along the longitudinal joint, as shown in Fig. 10.
- The neutral layer for the pavement is lower than the mid-depth plane of the PCC slab. This is due to the bonded or partially bonded interface condition between the PCC slab and the base layer.
- For the time being, most of the aircraft types in service still have a single main gear axle, like the B-727 and B-737 aircraft. For these aircraft types, the number of tensile strain repetitions on the top surface is double that of the number of tensile strains on the bottom surface.

In the current pavement design theories, the longitudinal and transverse strain components are believed to be similar based on the assumption of static symmetrical loaded area. This assumption has made the design process much simpler and more convenient. In reality, the transverse strain versus time curves and the longitudinal ones are not even close in shape. This discrepancy needs to be studied.

#### LOCATION OF MAXIMUM DEFLECTIONS AND STRAINS

As discussed previously, each deflection curve for the inner loading case has only one peak, no matter how

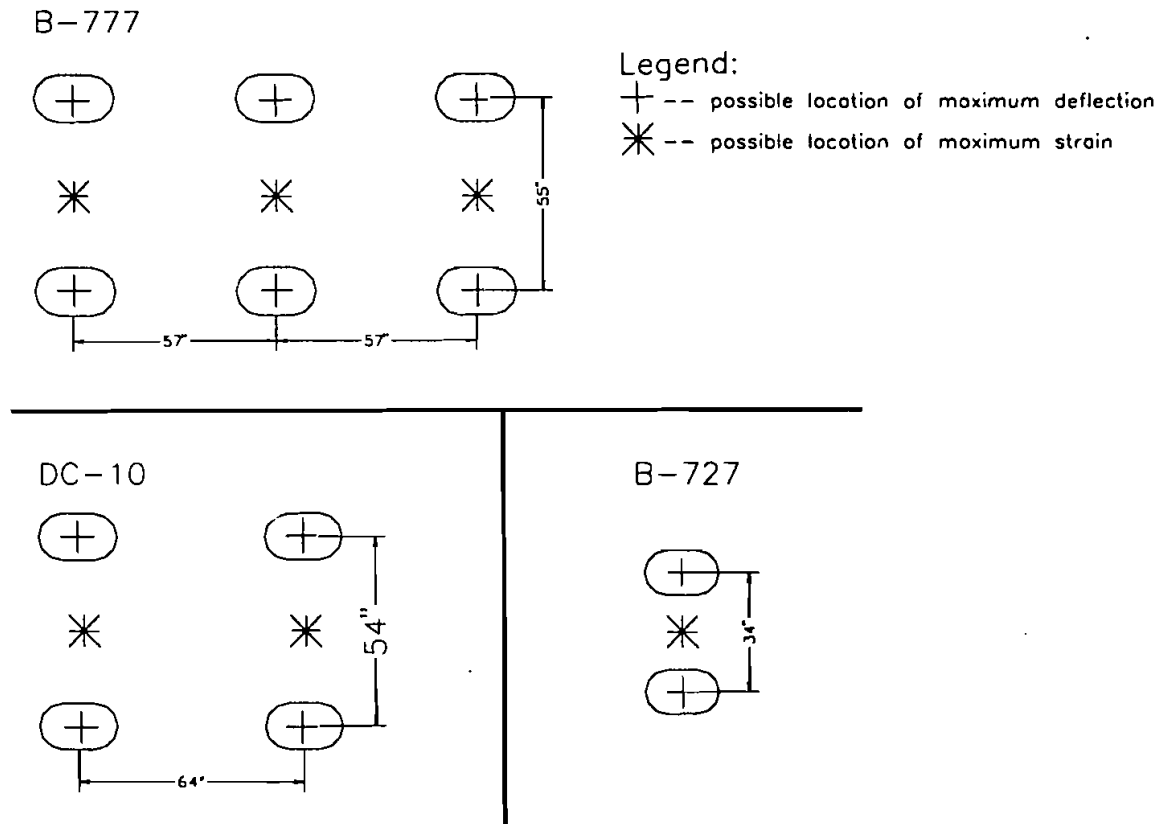


FIGURE 12 Critical deflection and strain locations for the edge loading case

many axles are on the main gear. However, each strain versus time curve in the same loading condition has the same number of peaks as the number of the main gear axles. To find out the exact critical deflection and location, the variation of deflection and strain values in the transverse direction are analyzed, as listed in Table II.

The comparison has proven that the deflection between the dual wheels of the aircraft gear is usually larger than the deflection beneath one of the wheels, but the larger strain value occurs right beneath the wheel rather than between the dual wheels. Based on the above analysis, the critical deflection and strain locations are depicted in Fig. 11.

Similarly, for the transverse joint, the possible critical deflections occur between the dual wheels and the possible critical strains for the three selected aircraft

types can be beneath any wheel on the main gear, as shown in Fig. 12.

## CONCLUSIONS

- The deflection versus time curve has one peak for the inner loading case and the same number of peaks as the number of the main gear axles for the edge loading case. The location of the peak for the inner loading case is at the geometric center of the semi-gear. The location of the maximum peak for the transverse edge loading case can be between any pair of the dual wheels, depending on the load transfer characteristics of the joint.
- The strain versus time curve has the same number of peaks as the number of the main gear axles for

both the inner loading case and the transverse edge loading case. The maximum strain peak can occur beneath any of the wheels on the main gear except for the inner loading case for the B-777 gear. In the later case, the maximum strain peak occurs beneath one of the dual wheels of the middle axle of the main gear.

- Curvature changes in the longitudinal strain versus time curves may cause fatigue initiated from the top surface of the pavement.
- Load transfer efficiency is dependent on the direction in which the aircraft is operated. The efficiency values decrease dramatically for undowelled dummy joints.

#### **Acknowledgements**

This work was completed at Galaxy Scientific Corporation under an FAA contract. I would like to express my sincere gratitude to the FAA Technical Center and Galaxy Scientific Corporation for their strong support during this study. The great help from Mr. Alex Ollerman on technical proofreading is also sincerely acknowledged.

#### **References**

- Dong, M., Hayhoe, G. and Fang, Y. (1997) Runway instrumentation at Denver International Airport: Dynamic sensor data processing *ASCE Airfield Pavement Specialty Conference, Seattle, Washington*, August 17-22.
- Internet Site <http://www.airtech.tc.faa.gov/pavement/projects/database.htm>, FAA Airport Technology Research and Technology Branch, AAR-410, William J. Hughes Technical Center, Atlantic City, New Jersey.